JOURNAL OF Materials CHEMISTRY

Evaluation of electrical polarizability and *in vitro* bioactivity of apatite $Sr_5(PO_4)_3OH$ dense ceramics

Hiroaki Takeda,† Yasuhiko Seki, Satoshi Nakamura and Kimihiro Yamashita‡

Institute of Biomaterials and Bioengineering, Tokyo Medical and Dental University, 2-3-10 Kanda-Surugadai, Chiyoda-ku Tokyo 101-0062, Japan

Received 4th March 2002, Accepted 22nd May 2002
First published as an Advance Article on the web 27th June 2002

Dense ceramics of $Sr_5(PO_4)_3OH$ (strontium hydroxide tris-phosphate with an apatite structure; Sr-HAp) with little dehydration were successfully synthesized in a humid atmosphere. Polarization of these Sr-HAp ceramics was performed by application of an external dc field at higher temperature. To clarify the polarization and depolarization phenomena of Sr-HAp, the polarized samples were analyzed by thermally stimulated depolarization current (TSDC) measurement. The features of the TSDC spectra were very similar to those of the isomorphic hydroxyapatite ($Ca_5(PO_4)_3OH$; HAp); moreover, the charges of sub-millicoulomb order could be stored in the polarized Sr-HAp. The results of *in vitro* characterization of polarized Sr-HAp ceramics were comparable to those observed on HAp with high biocompatibility, showing the acceleration of bone-like crystal growth on negatively charged ceramic surfaces by electrical polarization. These findings provide evidence that the surface charge of these apatite materials with hydroxide ions promotes the biological reaction.

Introduction

Hydroxyapatite ($Ca_5(PO_4)_3(OH)$; HAp) has been well developed as an implant material because of its outstanding biocompatiblity.[1] HAp also attracts great interest as a candidate for application to such fields as liquid chromatographic columns for the separation of proteins and nucleic acid, a catalyst for dehydration or dehydrogenation of some alcohols, powder carriers for removing heavy metal ions and chemical sensors for various gases.

Recently, we discovered that electrically polarized HAp had the ability to dominate the overgrowth of bone-like apatite crystals from simulated body fluid (SBF), depending on the polarity of the surface charges.[2] This ability is essentially useful to manipulate biomineralization, as has been pointed out in ref. 3. Using the polarized HAp ceramics, we also demonstrated remarkable biological responses; selective cell adhesion and growth,[4] and enhanced bone formation.[5] The superior bioactivity therefore will qualify the polarized HAp for use in a variety of applications in the biomaterial field, *i.e.*, tooth root and total hip joint replacement systems.

We have dealt with the polarization mechanism of HAp as well as the aforementioned biological and chemical effects. Our previous study revealed that the charges of microcoulomb order were stored in the polarized HAp.[6] Considering the activation energy for depolarization, we also proposed that the polarization of HAp was attributed to the migration of protons in the columnar OH^- channels with a micrometer-order distance. Although there are several reports that the polarization was caused by the effects of impurities and a phenomenon involving the monoclinic-hexagonal transformation,[7–13] we found no descriptions of the polarization mechanism of the large stored charge before our discovery. To determine whether isomorphic compounds of HAp have similar characteristics would be of importance for grasping the polarization mechanism. $Sr_5(PO_4)_3(OH)$ (abbreviated Sr-HAp) has been convenient for this purpose, because it has been reported that the polarization mechanism of this compound was comparable to that of HAp[8] and that selective cell adhesion on the polarized Sr-HAp was observed.[14] Moreover, the effects of strontium ions in glass-ionomer cements on the growth and dissolution of HAp and of strontium oxide on bone mineral detection were recently investigated in the biomaterial field.[15,16]

In the current work, dense Sr-HAp ceramics were first synthesized while preventing dehydration in the sintering process, because dense Sr-HAp has never been obtained because of the destruction of the apatitic structure arising from complete dehydration. Subsequently, the polarization and depolarization of sintered Sr-HAp ceramics were analyzed by thermally stimulated depolarization current (TSDC) measurements.[17] The larger stored charges of the ceramic Sr-HAp were discussed in relation to the thermal instability of these apatites. We also investigated the phenomenological effect of polarization on the bone-like crystal growth (actually partially carbonated calcium hydroxyapatite) on Sr-HAp ceramics. The results, in which both the TSDC profiles of Sr-HAp and the growth features were very similar to those observed on ceramic HAp, strongly advocated the proposed mechanisms for the polarization and depolarization of HAp and for the enhanced crystal growth.

Experimental

(1) Preparation of Sr-HAp dense ceramics

The powders of Sr-HAp were prepared by wet chemical synthesis using aqueous solutions of analytical grade $Sr(NO_3)_2$ and $(NH_4)_2HPO_4$. During synthesis, the pH of the reacting solutions was carefully kept at 10.5 using ammonia water in order to avoid the precipitation of $SrHPO_4$ as an impurity phase.[18] The reactant was treated by freeze drying for 24 h and calcination at 800 °C for 2 h. The calcined powders were found to consist of only the Sr-HAp phase using X-ray powder diffraction (XRD) measurements. The powders with a binder (2 wt% polyvinyl alcohol) were finely ground to under 200 mesh. The resulting powders were pressed uniaxially in disk form to 13 mm diameter and 1 mm thickness at about 220 Mpa. Dense Sr-HAp ceramics were made by sintering at 1250 °C for 2 h in saturated water vapor[19] or in air. The shape of these

†Present address: Graduate School of Materials Science, Nara Institute of Science and Technology (NAIST), 8916-5 Takayama-cho, Ikoma, Nara 630-0101, Japan. E-mail: hiro-t@ms.aist-nara.ac.jp
‡E-mail: yama-k.bcr@tmd.ac.jp

 DOI: 10.1039/b202262c

ceramics was disk-like of 11 mm in diameter and 1.0 mm in thickness.

The density of the Sr-HAp ceramics was measured by the Archimedes method using distilled water. The grain morphology of the ceramics was observed using scanning electron microscopy (SEM). XRD measurements of the Sr-HAp ceramics were carried out at room temperature. Infrared spectroscopic analysis of the Sr-HAp was done at room temperature with a JASCO FT-230 Fourier transform infrared spectrometer. The absorbance data for the Sr-HAp ceramics with KBr powder at a concentration of 1% were collected in the range of 400 to 4000 cm^{-1} at a resolution of 4 cm^{-1}.

(2) TSDC measurements

For the TSDC measurement, the specimens were disk-like shapes of 11 mm in diameter and 1.0 mm in thickness. Electrodes were prepared by painting a Pt paste on both sides of the specimens, followed by baking. During the polarizing procedure, the specimens were heated in air for the polarization time of 2 h (t_p) at the polarization temperatures (T_p) of 400 °C and thereafter cooled to room temperature (RT). The details of the polarization treatment are described in ref. 6. After the electrodes were short circuited at RT for a sufficient time, TSDC measurements were carried out in air from RT to 800 °C at a heating rate of 5.0 °C min^{-1}. The depolarization current was measured with a Hewlett-Packard 4140B pA meter.

(3) *In vitro* tests

In vitro tests were carried out by soaking the Sr-HAp ceramic specimens (disks of 10 mm in diameter and 0.7 mm in thickness) in a simulated body fluid (SBF),[20] which had inorganic ion concentrations equal to those of human blood plasma at pH 7.25 and 36.5 °C.

Before soaking in the SBF, the specimens were sandwiched between platinum electrode plates, heated to 400 °C in air, and electrically polarized in a dc field of 8.0 kV cm^{-1} for 2 h. The samples were then cooled to room temperature while being polarized. After the polarizing treatment, XRD measurement and infrared spectroscopic analysis were also performed. For the polarized Sr-HAp ceramics, the negatively and positively polarized surfaces were denoted as the N- and P-surfaces, respectively. The surfaces of the specimens without polarization were signified as the O-surface. These denotations have followed those used in the report on HAp ceramics (see ref. 2, 4, 5).

The specimens were removed from the SBF after soaking for 1–3 days, and their surfaces were studied by XRD and scanning electron microscopy coupled with energy dispersive spectroscopy (SEM-EDS) analysis.

Results

(a) Structural characterization of Sr-HAp dense ceramics

The relative density of the Sr-HAp ceramics was approximately 97%, a value which has never been reported. The grain size was identified to be 1–3 μm by SEM observation. Fig. 1 shows XRD profiles of Sr-HAp ceramics sintered at 1250 °C for 2 h under two kinds of atmosphere. The XRD profiles indicated that the Sr-HAp ceramics sintered in both saturated water vapor (Fig. 1a) and air (Fig. 1b) contained $Sr_3(PO_4)_2$ as an impurity phase. Sr-HAp ceramics sintered in saturated water vapor had a smaller amount of $Sr_3(PO_4)_2$ in contrast to those in air. The lattice parameters of Sr-HAp were $a = 0.9771(1)$, $c = 0.7289(1)$ nm, which were determined using 2θ values of the corresponding peaks. The lattice parameters were consistent with those[18] previously reported ($a = 0.976$, $c = 0.728$ nm).

The infrared spectrum of the Sr-HAp ceramics sintered in saturated water vapor at 1250 °C is shown in Fig. 2. The peaks

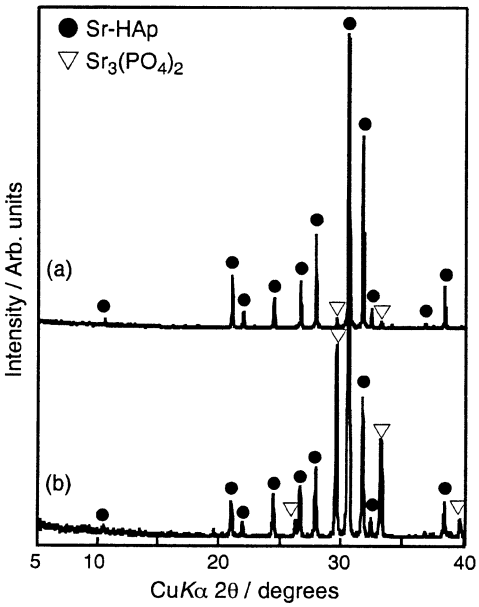

Fig. 1 XRD profiles of Sr-HAp ceramics sintered at 1250 °C for 2 h in saturated water vapor (a) and in air atmosphere (b).

assigned to the stretching and bending absorption of the hydroxide ions were observed at 3570 and 630 cm^{-1}, respectively. The broad absorption bands at 3400 and 1650 cm^{-1} were ascribed to adsorbed water molecules. For the Sr-HAp ceramics sintered in air, those peaks assigned to the hydroxide ions were not observed. These absorption intensities were apparently smaller compared with those of HAp[6,21] but were as strong as those of pure Sr-HAp powders prepared without heat treatment.[22] Moreover, it was reported that the absorption intensities assigned to the hydroxide ions were reduced with increasing Sr-content (x) in the solid solution $Ca_{5-x}Sr_x(PO_4)_3(OH)$.[23] These observations indicated that the current Sr-HAp ceramics sintered in saturated water vapor contained hydroxide ions in the structure. For TSDC measurements and *in vitro* tests described below, Sr-HAp ceramics sintered in saturated water vapor were used.

(b) Thermal depolarization

The effect of the electrical field strength (E_p) of the Sr-HAp ceramics on the TSDC spectra is shown in Fig. 3, while the polarization temperature (T_p) and time (t_p) were 400 °C and 2 h, respectively. All of the TSDC curves of the polarized Sr-HAp ceramics increased at about 140 °C, reached maximum points, and then gradually became attenuated. The peak temperature (T_{peak}) of the TSDC curves decreased with an increment in the applied electrical field strength. The maximum

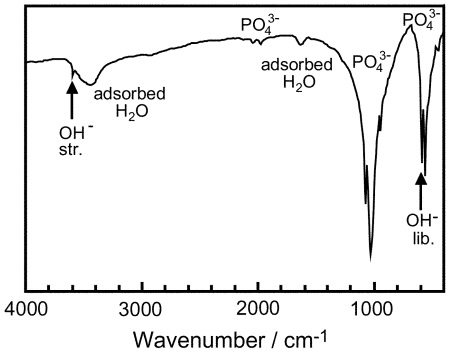

Fig. 2 IR spectrum of Sr-HAp ceramics sintered at 1250 °C for 2 h in saturated water vapor. Arrows indicate peaks assigned to absorption bands of hydroxide ions.

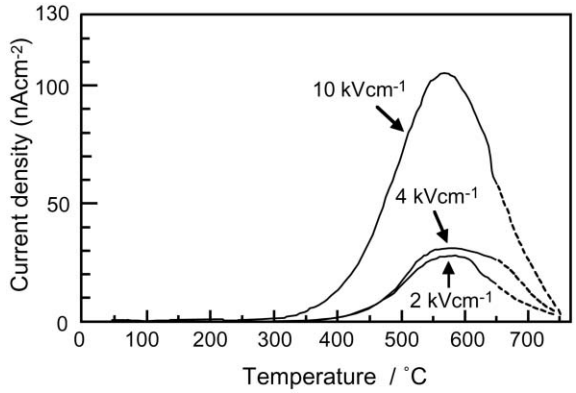

Fig. 3 TSDC spectra of Sr-HAp ceramics polarized in dc fields of 2, 4, and 10 kV cm^{-1} for 2 h at 400 °C. Heating rate was 5 °C min^{-1}.

current density (J_{max}) of the Sr-HAp polarized at 4 and 10 kV cm^{-1} was 1.3 and 4.3 times larger than that at 2 kV cm^{-1}, respectively. The result that J_{max} increased with increasing electrical field strength was identical to that obtained with HAp. The values of the polarization charge (Q_p) were calculated from the TSDC spectra using the equation

$$Q_p = \frac{1}{\beta}\int J(T)\mathrm{d}T \quad (1)$$

where $J(T)$ is the measured discharge current density at a temperature T and β is the heating rate. Because each $J(T)$ did not reach 0 below 650 °C, $J(T)$ was linearly extrapolated over this temperature. The calculations are shown in Table 1, involving the corresponding data of HAp. The difference in the TSDC curves between Sr-HAp and HAp will be discussed further below.

(c) Changes in the surface of the Sr-HAp ceramics after soaking in SBF

Fig. 4 shows SEM micrographs of the O-, N-, and P-surfaces of Sr-HAp ceramics after 1-day and 3-day immersions in SBF. Grainboundaries are clearly seen on the O- and P-surfaces of the Sr-HAp ceramics after 1-day immersion (Fig. 4(a_1) and 4(c_1)). On the other hand, indistinct grainboundaries and small particles with a dimension of ~0.5 μm were observed on the N-surface (Fig. 4(b_1)). After 3-day immersions, the O- and P-surfaces of the Sr-HAp ceramics hardly changed (Fig. 4(a_2) and 4(c_2)) and still showed clear grainboundaries. The N-surface of the Sr-HAp ceramics after 3-day immersions is completely covered with the layers precipitated from SBF, as seen in Fig. 4(b_2). Furthermore, there are some aggregates composed of round particles of 2 to 3 μm in diameter on this N-surface. A magnified micrograph of the aggregate is presented in Fig. 5. The EDS profile of this aggregate on Sr-HAp ceramics is also included. In the sample, Ca and P were observed, and a small amount of Na was also detected. The Au detected was from the sputtered films used for the SEM observation, and Sr from the Sr-HAp ceramics. Both the layers and the aggregates consist of numerous needles and were identical to that of bone-like crystals in shape.[20] These SEM observations and the EDS results showed that the layers and the aggregates deposited were bone-like crystals. Therefore, it was revealed that the growth of the bone-like crystals was accelerated on the N-surface of Sr-HAp ceramics.

Discussion

(a) Structural consideration of depolarization

As shown above, a humid atmosphere was effective in preventing dehydration in the preparation of Sr-HAp ceramics at high temperature; the ceramics sintered in the water vapor at 1250 °C still had a small amount of the $Sr_3(PO_4)_2$ phase. The $Sr_3(PO_4)_2$ phase forms through the pyrolysis of Sr-HAp, accompanying the dehydration. On the other hand, there is no impurity phase in the HAp ceramics synthesized under the same conditions used in this study.[6] It was reported that few hydroxide ions were observed in HAp sintered at 1350 °C in air, but the HAp remained stable with decomposition of the apatitic structure.[21] This means that the hydroxide ions in HAp are rather highly mobile, namely, that OH^- diffusion in HAp occurs easily without skeletal destruction. The lattice hydroxide ions exist in the columnar channel by forming one-dimensional chains parallel to the crystallographic *c*-axis.[24] Based on these results, we corroborated the belief that Sr-HAp was thermally unstable in contrast to HAp and then suggested that OH^- diffusion in Sr-HAp occurred with difficulty and led to the decomposition of its own structure.

All TSDC curves of the Sr-HAp ceramics had broad peaks. The peak temperature (T_{peak}) giving the maximum current decreased from 580 to 568 °C with an increment in the external field intensity. These observations were similar to those obtained with HAp.[6–8] Thus, this suggested that the polarization of Sr-HAp also involved ion transport. In the reports using a thermal sampling method,[8] three kinds of depolarization relaxation of Sr-HAp occurred at 225, 362, and 725 °C. The relaxation at 225 and 362 °C was attributed to the proton rotation of OH^- in the columnar channels with regard to the monoclinic-hexagonal transformation, but that at 725 °C could be not interpreted. The T_{peak} observed in the present study was close to the highest temperature (725 °C). The thermal depolarization of Sr-HAp was found from the TSDC measurement to start at 140 °C. This indicated that the proton rotation contributed to the polarization and depolarization. However, the $J(T)$ values corresponding to the depolarization by proton re-rotation were negligibly small compared with those obtained at T_{peak} (in the case of E_p = 2 kV cm^{-1}, 0.08, 0.38, and 28.6 nA cm^{-2} at 225, 362, and 580 °C, respectively). It was certain, therefore, that the depolarization mechanism of the polarized Sr-HAp ceramics was ionic transport.

The possible carriers producing the ion transport in the Sr-HAp ceramics were (i) the OH^- and (ii) H^+ ions in the OH^- columnar channels. We identified the ion carrier by determining the activation energy related to the depolarization relaxation of Sr-HAp, as is the case for HAp.[6–8,13] Using the results of our TSDC spectra, we can calculate the activation energy from the Arrhenius plots obtained. The relaxation time τ can be described by the following equation:

Table 1 Effects of polarization conditions on the polarization charge (Q_p) obtained from TSDC spectra, and the activation energy (H) of depolarization of Sr-HAp and HAp ceramics

Ceramics	Polarization			Depolarization			
	T_p/°C	E_p/kV cm^{-1}	t_p/h	T_{peak}/°C	J_{max}/nA cm^{-2}	Q_p/μC cm^{-2}	H/eV
Sr-HAp	400	2	2	580	28.6	60	0.66
	400	4	2	575	31.2	81	0.72
	400	10	2	568	106.3	260	0.68
HAp[a]	400	1.0	1	420	7.87	14.9	0.84

[a]After ref. 6.

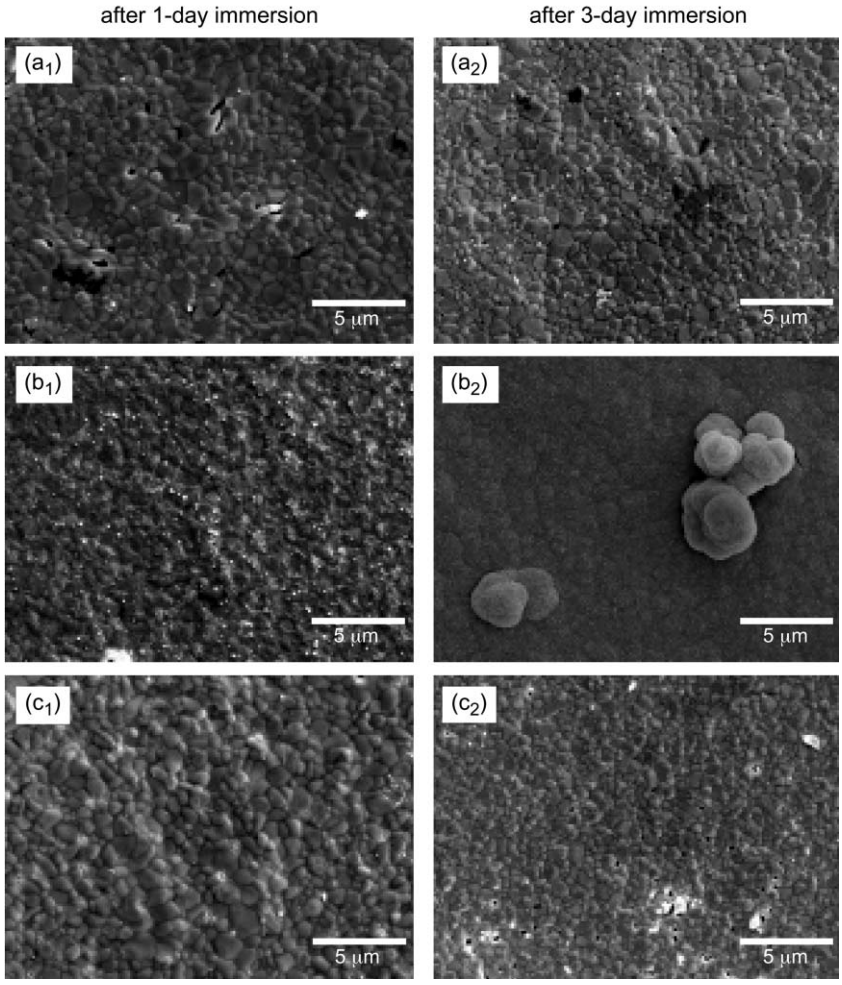

Fig. 4 SEM photographs of O- (a), N- (b), and P- surfaces (c) of Sr-HAp ceramics after 1-day (a_1, b_1, c_1) and 3-day (a_2, b_2, c_2) immersions in SBF.

$$\tau(T) = \tau_0 \exp\left(\frac{H}{kT}\right) = \frac{1}{\beta J(T)} \int_T^{\infty} J(T)\mathrm{d}T \qquad (2)$$

where H is the activation energy, τ_0 is a pre-exponential factor, and k is Boltzmann's constant. Fig. 6 shows the $\ln \tau(T)$ *vs.* $1/T$ plots, the so-called the Arrhenius plots, produced from the TSDC curves data, analyzed with the help of eqn.(2). By fitting linear lines to the plots for Sr-HAp polarized in dc fields of 2, 4, and 10 kV cm^{-1}, the slopes of H/k were obtained as a function of T. The activation energies calculated by the least squares method are shown in Table 1. The activation energies for the depolarization relaxation were 0.66–0.72 eV for the Sr-HAp polarized in this study. These values agreed well with those (0.6 ± 0.1 eV) of the proton migration along the OH^- chain in

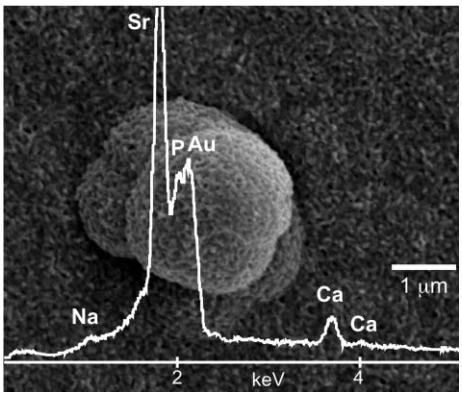

Fig. 5 SEM photograph and EDS profile of the N-surface of the Sr-HAp ceramic after 3-day immersion in SBF.

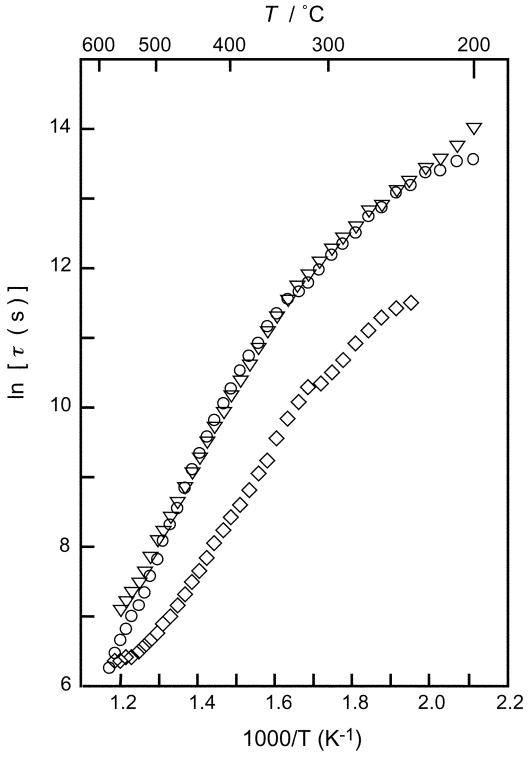

Fig. 6 $\ln\tau$ *vs.* $1/T$ for Sr-HAp according to eqn.(2). Data points were plotted using TSDC curves of specimens polarized in dc fields of 2 (▽), 4 (○), and 10 (◇) kV cm^{-1} at 400 °C.

the pure HAp structure estimated from the conductivity measurements with H_2 gas pulsed supplements.[25] Moreover, the activation energies of the OH^- diffusion were 230 $\pm$ 15 kJ mol^{-1} (2.38 $\pm$ 0.16 eV),[26] which were obtained from the crystallization process of the amorphous phase of HAp, were three times those in the present study. These results revealed that the polarization of Sr-HAp was ascribed to the migration of protons in the columnar OH^- channels.

The TSDC curves for Sr-HAp and HAp[6] were similar in shape, but different in the peak temperature (T_{peak}) and the amount of polarization charges (Q_p). As shown in Table 1, the T_{peak} of the Sr-HAp polarized sample was *ca.* 160 °C higher than that of the HAp. This tendency was also observed in the reports using the thermal sampling method.[8] In the report, it was assumed that the elevation of this relaxation temperature was due to reduction of the Me^{2+} (Me = Ca, Sr) triangle's "tunnel size", which was there defined as the distance from the center (6_3 axis) to the Me^{2+} ion center minus the ion radius (see Fig. 7). It was proposed that the tunnel size reduced by Sr^{2+} substitution for Ca^{2+} would make it more difficult for the H^+ to rotate around the O^{2-}, thus leading to a higher relaxation temperature.[8] This proposal was also suitable for our model in which the polarization of apatites including hydroxide ions was attributed to the migration of protons in the columnar OH^- channels. The reason was that the proton conduction along the columnar OH^- channels was always accompanied by the proton rotation from the initial position to the position on the opposite side through the Me^{2+} triangle, as demonstrated in ref. 6. By the way, although this proton conduction required the proton vacancies of the O^{2-} in OH^- ions, these vacancies were confirmed to exist in HAp heated to over 1000 °C in air.[21]

The difference in Q_p between Sr-HAp and HAp was not discussed in the present study, because the polarization conditions of these two apatites were different. The maximum Q_p for the Sr-HAp polarized at 400 °C under 10 kV cm^{-1} was of sub-millicoulomb order, as shown in Table 1. We expect that Q_p values of the same order are also obtained for the HAp ceramics if polarized under stronger polarization fields at higher temperature. Further investigations are now in progress.

(b) An explanation of the accelerated growth phenomena on the N-surface

The accelerated growth of bone-like crystals was observed only on the N-surface of polarized Sr-HAp ceramics, whereas no crystal growth ever took place on the O- and P-surfaces even after a 3-day immersion in SBF. These observations are analogous to those on polarized HAp ceramics in 1.5SBF,[2] which has 1.5 times the inorganic ion concentrations of the SBF used in this study. The accelerated and decelerated growth phenomena on polarized HAp ceramics in 1.5SBF were well explained as follows:[2]

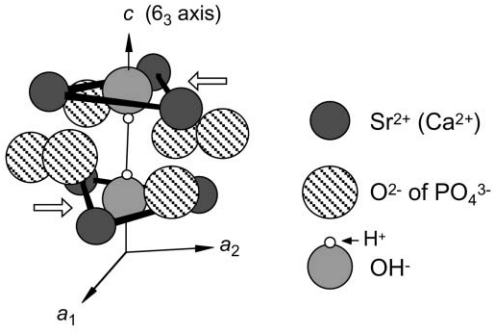

Fig. 7 Schematic illustration of the atomic environment around OH^- ions in the apatitic structure. Open arrows (⇒) guide the Sr (Ca) triangles which are made by connecting three of six equivalent Sr (Ca) ions placed at z = 1/4.

(i) On the N-surface, metallic cations (Ca^{2+}, Mg^{2+} and Na^+) in SBF are more rapidly adsorbed than on other surfaces. Nucleation takes place among these supersaturated ionic groups, and the remaining dipole moments accelerate the growth of nuclei due to the attraction of these ions.

(ii) On the P-surface, anions (chloride, phosphate and carbonate) appear to be mainly adsorbed, which may be unfavorable for crystal growth.

The former model could be demonstrated by our results on the N-surface of polarized Sr-HAp ceramics. Unfortunately, the latter results were not supported because there was no difference between the P- and O-surfaces in the crystal growth. Thirty days were needed to grow the crystal layers from SBF on as-sintered, that is, non-polarized, HAp ceramics.[27] Use of 1.5SBF or a longer immersion period in SBF was found to be necessary to confirm the deceleration effect on the P-surface. The SEM observation on the N-surface clearly showed that the bone-like crystals had already grown after 1-day immersions in SBF (Fig. 4(b_1)), disclosing a substantial acceleration effect due to the polarization. These findings have provided evidence that the surface charge can control the biological reaction.

Conclusion

In this study, TSDC measurements and *in vitro* tests were performed using dense Sr-HAp ceramics with little dehydration. Based on the present TSDC study, it was demonstrated that the polarization of Sr-HAp ceramics was attributable to the transportation of the protons in the OH^- columnar structure, as was observed with HAp ceramics. Moreover, taking into consideration the higher mobility of protons in the columnar structure of Sr-HAp, we indicated that the larger polarization charges for Sr-HAp ceramics could be stored. The *in vitro* study of the polarized Sr-HAp ceramics substantiated that the negatively charged surfaces of the polarized HAp ceramics accelerated the growth of bone-like crystals.

Acknowledgement

The authors wish to thank Dr. Masataka Ohgaki and Ms. Akiko Obata of the Institute of Biomaterials and Bioengineering, Tokyo Medical and Dental University, for their help in carrying out the *in-vitro* test and TSDC measurements. This work was partly supported by Grants-in-Aid for General Scientific Research (A)-10305047 and (C)-11650855 from the Ministry of Education, Culture, Sports, Science and Technology of the Japanese Government.

References

1 L. L. Hench, *J. Am. Ceram. Soc.*, 1998, **81**, 1705.
2 K. Yamashita, N. Oikawa and T. Umegaki, *Chem. Mater.*, 1996, **8**, 2697.
3 P. Calvert and S. Mann, *Nature*, 1997, **386**, 127.
4 M. Ohgaki, T. Kizuki, M. Katsura and K. Yamashita, *J. Biomed. Mater. Res.*, 2001, **57**, 366.
5 T. Kobayashi, S. Nakamura and K. Yamashita, *J. Biomed. Mater. Res.*, 2001, **57**, 477.
6 S. Nakamura, H. Takeda and K. Yamashita, *J. Appl. Phys.*, 2001, **89**, 5386.
7 N. Hitmi, D. Chatain, C. LaCabanne, J. Dugas, J. C. Trombe, C. Rey and G. Montel, *Solid State Commun.*, 1980, **33**, 1003.
8 N. Hitmi, C. LaCabanne and R. A. Young, *J. Phys. Chem. Solids*, 1986, **47**, 533.
9 N. Hitmi, E. Lamure-Plaino, C. LaCabanne and R. A. Young, *Calcif. Tissue Int.*, 1986, **38**, 252.
10 B. S. H. Royce, *Ann. N.Y. Acad. Sci.*, 1974, **238**, 131.
11 J. C. Elliott and R. A. Young, *Bull. Soc. Chim. Fr.*, 1968, **180**, 1763.
12 J. Arends, B. S. H. Royce, J. Siegel and R. Smoluchowski, *Phys. Lett. A.*, 1968, **27**, 720.
13 A. Bennis, F. Miskane, N. Hitmi, M. Vignoles, M. Heughebaert,

A. Lamure and C. LaCabanne, *IEEE Trans. Electr. Insul.*, 1992, **27**, 826.
14 Y. Seki, M. Ohgaki, S. Ichinose, T. Tsuchiya and K. Yamashita, in *Bioceramics* **Vol. 12**, ed. H. Ohgushi, G. W. Hastings, and T. Yoshikawa, World Scientific, Singapore, 1999, p. 105.
15 S. Deb and J. W. Nicholson, *J. Mater. Sci. Mater. Med.*, 1999, **10**, 474.
16 J. Christoffersen, N. M. Christoffersen, N. Kolthoff and O. Bärenholdt, *Bone*, 1997, **20**, 47.
17 C. Bucci and R. Fieschi, *Phys. Rev. Lett.*, 1964, **12**, 16.
18 S. Kurata, T. Fujiwara and H. Negishi, *Jpn. J. Oral Biol.*, 1982, **24**, 661 [in Japanese].
19 K. Yamashita, K. Kitagaki and T. Umegaki, *J. Am. Ceram. Soc.*, 1995, **78**, 1191.
20 T. Kokubo, H. Kushitani, S. Sakka, T. Kitsugi and T. Yamamoto, *J. Biomed. Mater. Res.*, 1990, **24**, 721.
21 C.-J. Liao, F.-H. Lin, K.-S. Chen and J.-S. Sun, *Biomaterials*, 1999, **20**, 1807.
22 M. Aizawa, F. S. Howell and K. Itatani, *J. Ceram. Soc. Jpn.*, 1999, **107**, 1011.
23 M. Andres-Verges, F. J. Higes-Rolando and P. F. Gonzalez-Diaz, *J. Solid State Chem.*, 1982, **43**, 237.
24 M. I. Kay, R. A. Young and A. S. Posner, *Nature*, 1964, **204**, 1050.
25 G. C. Maiti and F. Freund, *J. Chem. Soc., Dalton Trans.*, 1981, **6**, 949.
26 K. A. Gross, V. Gross and C. C. Berndt, *J. Am. Ceram. Soc.*, 1998, **81**, 106.
27 T. Kokubo, H. Kushitani, Y. Ebisawa, T. Kitsugi, S. Kotani, K. Oura and T. Yamamuro, in *Bioceramics*, **Vol. 1**, ed. H. Oonishi, H. Aoki and K. Sawai, Ishiyaku EuroAmerica, Tokyo, 1989, p. 157.